# THE HYPERPOLARIZING REGION OF THE CURRENT-VOLTAGE CURVE IN FROG SKIN

OSCAR A. CANDIA

*From the Department of Ophthalmology, Mount Sinai School of Medicine of the City University of New York, New York 10029*

ABSTRACT Excitability (action potential and refractory period) has been described by A. Finkelstein in the depolarizing region of the current-voltage (*I-V*) curve of the isolated frog skin. Recently Fishman and Macey interpreted this phenomenon as a consequence of a region with negative resistance that confers to the *I-V* curve an N shape. We have studied the *I-V* relation of the isolated frog skin in the hyperpolarizing region with a current-ramp system. It was found that in $Na_2SO_4$ Ringer's, the resistance continuously increases in the hyperpolarizing direction. When hyperpolarization reaches 300 mv an electrical breakdown occurs, occasionally followed by a region of negative resistance. In NaCl Ringer's the breakdown was also found although the *I-V* relation was reasonably linear. Unidirectional $Na^+$ outflux was measured at different levels of voltage clamping across the skin and with different $Na^+$ concentrations in the solutions. The $Na^+$ outflux was found to be relatively independent of these parameters. Based on these results a $Na^+$ rectifying structure is postulated. An electrical model for active $Na^+$ transport including a diode and an oscillator is proposed. The effects of $CO_2$, nitrogen, amiloride, and ouabain on the *I-V* relation are described.

## INTRODUCTION

The isolated frog skin has been used for many years as a model for the study of ionic transport. The membrane is usually represented by an electrical circuit consisting of an emf and linear resistors. It is generally accepted that the computation of the electrical resistance from potential difference (PD) and short-circuit current (SCC) is valid since the resistance seems to be a linear parameter within this range. Linderholm (1) has reported that the electrical DC conductance of frog skin is essentially equal to the conductance of $Cl^-$ plus $Na^+$ ions. Brown and Kastella (2) have made impedance measurements in frog skin and have also reported linear behavior.

Excitability in frog skin was reported by Finkelstein (3, 4) who described an action potential of about 200 mv and 10 msec. This action potential occurs when current is sent in the depolarizing direction and occasionally with a hyperpolarizing current.[1] Finkelstein had interpreted this action potential as the result of a time vari-

[1] In the isolated frog skin the inside (connective side) is spontaneously positive with respect to the outside (cornified side). When positive current is sent through the skin from the outside to the inside

ant resistance element. The anatomical origin of this action potential has been clarified by the work of Lindeman and Thorns (5) and Fishman and Macey (6) who provided different evidence indicating that the spike is generated in the outermost cell membrane of the epidermis. Excitability has also been described in the toad bladder by Finkelstein and in the isolated skin of the toad *Bufo arenarum Hensel* by Bueno and Corchs (7).

Recently, Fishman and Macey (8, 9, 10) have used a fast voltage-clamp system to determine the current-voltage (*I-V*) relation in the depolarizing region of the isolated frog skin. Step and ramp voltage-clamp measurements showed the presence of an N-shaped *I-V* curve. An incremental limited "negative resistance" region and a subsequent breakdown confers the N shape to the *I-V* curve. Fishman and Macey suggested that the excitability in frog skin is a manifestation of such time varying negative resistance.

These studies have provided new information and a more precise description of the electrical properties of frog skin. However, they have not appreciably contributed to a better understanding of the mechanism of active transport of sodium in frog skin. Fishman and Macey also concluded that there is no direct connection between excitability and the "Na pump" in frog skin.

Study of the *I-V* curve in skin has been confined to the depolarizing region and little attention has been given to the hyperpolarizing region. In *Nitella* and *Chara australis*, Coster (11) has determined the *I-V* curve in the hyperpolarizing region. He shows that the system displays rectification and in many respects is similar to a solid-state p-n junction. In the case of reversed bias, namely hyperpolarization, an electical breakdown occurs which is referred to as the "punch-through" effect.

The purposes of this study are (*a*) to describe a nonlinear behavior of both $Na^+$ fluxes and the *I-V* curve of frog skin in the hyperpolarizing region; and (*b*) to emphasize the similarities between the *I-V* curve in frog skin and that of a structure with a p-n junction properties.

A model of ionic transport for frog skin incorporating a p-n type junction can explain certain electrical properties of the Na pump not predicted in the classical model of transport devised by Koefoed-Johnsen and Ussing. Since the *I-V* curve described by Coster (11) in *Nitella* is very similar to the one we found in the frog

---

this PD is first decreased, then brought to zero (SCC point), and eventually reversed. Current in this direction is called depolarizing current and the region of the *I-V* plane defined by this direction of current is called depolarizing region.

Conversely, positive current sent through the skin from inside to the outside increases the spontaneous PD. Current in this direction is called hyperpolarizing current and the region of the *I-V* plane defined by this direction of current is called hyperpolarizing region.

For practical reasons related to the way that our recording equipment was designed, *V* will be represented on the *Y* axis and *I* on the *X* axis. Also, the outside of the skin will be considered as reference side, so that the spontaneous PD will be on the positive side of the *V* axis. Hyperpolarizing current will be on the positive side of the *I* axis and depolarizing current on the negative side, so the SCC will be a negative current.

skin, it is possible that our model could have a more general application. It could also provide insight as to some of the aspects of $Na^+$ transport and to the effects of pharmacological agents presently not clearly understood.

## METHODS

### *General*

Experiments to be described were performed in vitro using the abdominal skin of the frog *Rana catesbeiana*, and on some occasions, the skin of *Rana pipiens*. Results from these two animals showed no essential differences. After isolation from the animal, the skin was mounted between two Ussing-type Lucite half-chambers. Two types of chambers were used; (*a*) a one compartment conventional chamber with a cross-sectional area of 3.5 $cm^2$; and (*b*) a four compartment chamber with a cross-sectional area of 2 $cm^2$ for each compartment (Fig. 1). All four compartments have a cylindrical shape and were electrically isolated from one another. This chamber permitted us to make four simultaneous experiments on the same skin. The chambers have outlets to connect PD and current electrodes. PD electrodes consisted of polyethylene tubing filled with agar-Ringer's connected to calomel electrodes. Current electrodes consisted of a thick disc of agar-Ringer's filling the closed end of the chamber's compartment. One side of the disc was in contact with the solution bathing the skin and the other with a small reservoir containing Ringer's with a platinum wire immersed into it. Solutions in the chamber were circulated and aerated by bubbling air (or other gas, as specified). The skin was bathed in a Ringer's solution with the following basic composition: $Na^+$ 103.5 mM, $K^+$ 3.0 mM, $Mg^{++}$ 1.2 mM, $Ca^{++}$ 1.0 mM, $Cl^-$ 75.0 mM, $HCO_3^-$ 25.0 mM, $SO_4^{--}$ 1.8 mM, $HPO_4^{--}$ 2.3 mM, $H_2PO_4^-$ 0.7 mM, gluconate$^{--}$ 1.0 mM, glucose 26.0 mM. When the effect of replacement of ions was studied, chloride was substituted by sulfate and sodium by choline. Osmolarity was compensated for with sucrose if necessary. The pH of the solution was about 8.6, except when $CO_2$ was bubbled, in which case the pH was about 6.2.

### *Determination of Resistance Curves*

Two types of current clamps were used for the determination of the *I-V* curves. (*a*) A slow current ramp (about 6 $\mu$a increment per sec per $cm^2$ of membrane). (*b*) A fast current ramp (in a range from 0.015 to 7.580 $\mu$a increment per msec per $cm^2$ of membrane).

(*a*) In the slow current-clamp ramp (Fig. 2) the potential electrodes were connected to a voltage recorder (*Y* axis). Each current electrode was connected to the positive output of a different constant-current source. The negative outputs of both current sources were connected to the center contact of a 10-turn potentiometer (10-T-P). The amount and direction of current delivered to the membrane is controlled by the 10-T-P in parallel to the membrane and to the current sources. The position of the center contact of the 10-T-P is linearly related to the amount of current sent across the membrane. The current sources can be balanced so that, when the center contact of the 10-T-P is in the middle of its run, no current is sent to the membrane. This arrangement permits sending to the membrane a continuously decreasing depolarizing current followed without interruption by a continuously increasing hyperpolarizing current and vice versa. The center contact of the 10-T-P is mechanically coupled the chart motor of the recorder. In this manner the *X* axis of the recorder is linearly related to the current sent across the membrane and the recorder will record a voltage-current relation, the slope of this curve being the resistance of the membrane. The recorder used was a Heath EUW-20A (Heath Company, Benton Harbor, Mich.) with a reversible chart motor. The recorder's chart motor controlled the ramp. The circuitry of the constant-current source

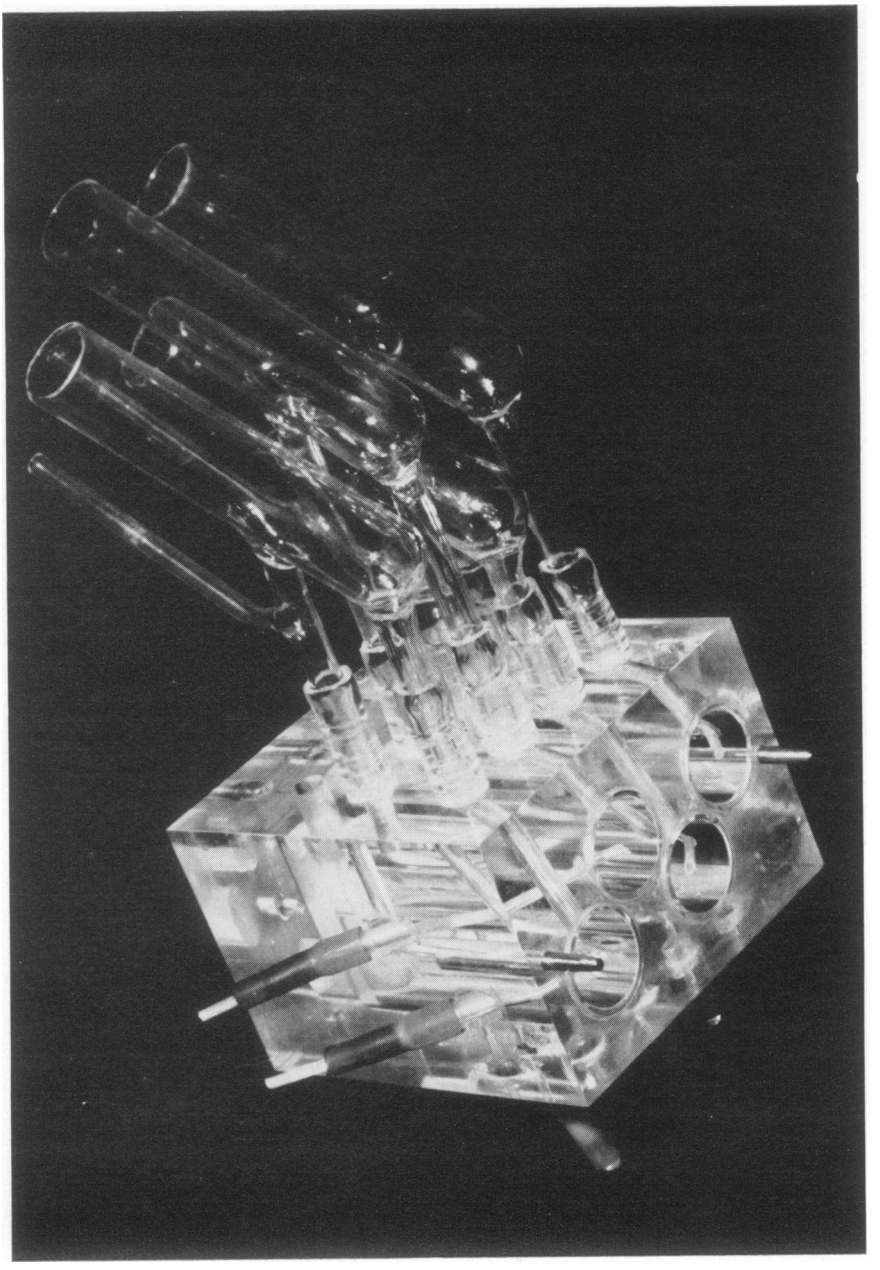

FIGURE 1 Photograph of one side of the four compartment Lucite chamber. Polyethylene PD electrodes are inserted in the chamber. Connected to the chamber is glassware for the circulation of Ringer's and gas bubbling.

and 10-T-P arrangement used here as part of the current ramp is described by Candia (12) elsewhere.

(*b*) The fast current-clamp ramp is shown by a schematic diagram in Fig. 3. The potential electrodes were connected to a DC high impedance probe (Nos. 1 and 2 in Fig. 3, Grass

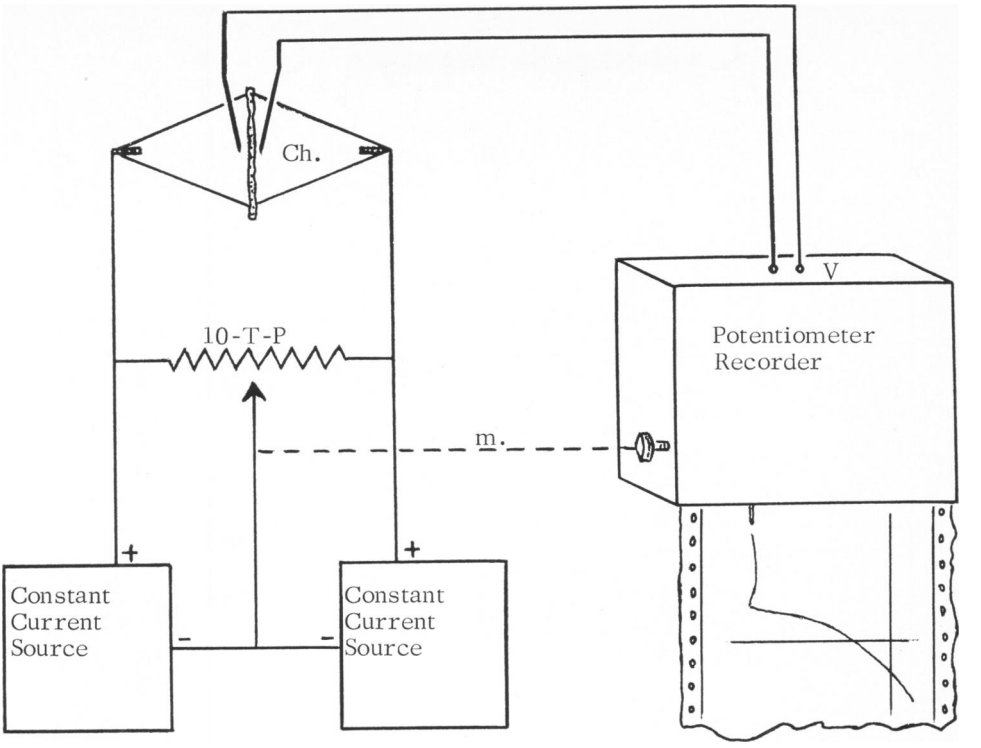


FIGURE 2 Schematic diagram of the current-ramp device. Ch.: chamber with skin. Potential electrodes are connected to *V*, voltage input of the recorder. 10-T-P: 10-turn potentiometer, the center contact of which is mechanically coupled by m to the recorder.

model P 17 [Grass Instrument Co., Quincy, Mass.], independent input impedance equal to $10^{11}$ Ω with field effect transistor [FET] circuits). The P17 is used as an impedance matching device and is connected to a Philbrick P 2A (No. 3 in Fig. 3) differential operational amplifier (Philbrick/Nexus Research, Dedham, Mass.). The P 17 with the P 2 A makes up a high-input impedance differential-to-single-ended amplifier with an over-all gain of one. Output of amplifier 3 was connected to amplifier 4 (one unit of a Health EUW-19B). It was used as an inverter and to get a potential gain of ten. Amplifier 4 could be omitted depending upon the gain characteristics of the oscilloscope. The output of amplifier 4 was fed to the vertical input of a Tektronix 564 B storage oscilloscope (Tektronix, Inc., Beaverton, Ore.).

The current-ramp pulse is originated in a sweep circuit. It consists of a FET operating as a constant-current source.[2] The constant current charges up a capacitor in the sweep circuit linearly with time and produces a concomitant voltage signal between amplifier 5 and the junction *a*. Upon reaching the end of its linear excursion the signal is returned rapidly to zero. The signal is fed to a follower amplifier (No. 5). The output of this amplifier is connected to the control amplifier (No. 6) and booster amplifier (No. 7). The current through the skin is sent across the resistor $R_1$ and fed to amplifier 8. The voltage output of this amplifier which is proportional to the current in $R_1$ is connected to the horizontal input of the Tektronix 564 B oscilloscope. The slope of the beam trace in the oscilloscope screen is proportional to

[2] FET's in solid-state timers, File 104, May, 1965. Siliconix Incorporated, Sunnyvale, Calif.

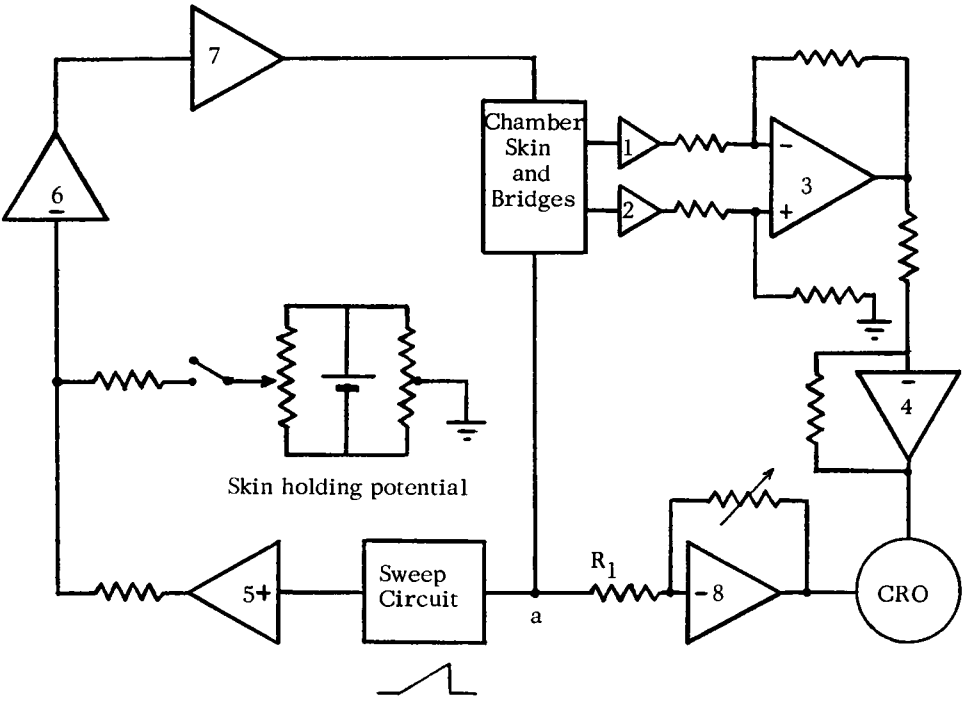


FIGURE 3 Schematic diagram of the fast current-ramp system. See description in text.

the skin's resistance. Photographs of the *I-V* curves were obtained with a C 12 Polaroid camera (Polaroid Corp, Cambridge, Mass.) attached to the scope.

Amplifiers 4–8 were part of a EUW-19B operational amplifier system. They were stabilized with a Heath EUA-19-4 stabilizer. The rise time of the amplifiers is 12 $\mu$sec. Linearity in the system was controlled by replacing the skin with a dummy membrane.

Voltage across resistor $R_1$ is equal to signal $V$ in the sweep circuit. The loop current $I_1$ is given by: $I_1 = V/R_1$. The timing period, in seconds, to change the signal from 0 to $V$ is given by: $t = CV/I_d$, where $C$ is capacitance in $\mu$F, $V$ in volts, and $I_d$ (the drain current) in $\mu$a. By combining the last two equations, the rate of increment of the loop current per unit of time can be obtained; $I_1/t = I_d/R_1C$. $I_d$ and $C$ are variables in the sweep circuit.

### *Measurement of Unidirectional Sodium Fluxes*

Unidirectional sodium outflux (inside to outside) was measured in $Na_2SO_4$ Ringer's solution at three levels of voltage clamping: +60, 0, and −60 mv. $Na^{22}$ was added to the inside bathing solution. Specific activity in this side was kept constant throughout the experiment. Samples were taken from the outside bathing solution at 30-min intervals. Radioactivity in the outside solution was less than 5% of the activity in the inside solution. Samples were counted with a Packard auto-gamma Spectrometer (Packard Instrument Co., Downers Grove, Ill.). At least three 30 min flux periods in each of the three potential levels were measured in the same skin. In other experiments sodium outflux was measured in the same skin before and after the sodium concentration was changed in both bathing solutions from 104 mM to 31 mM.

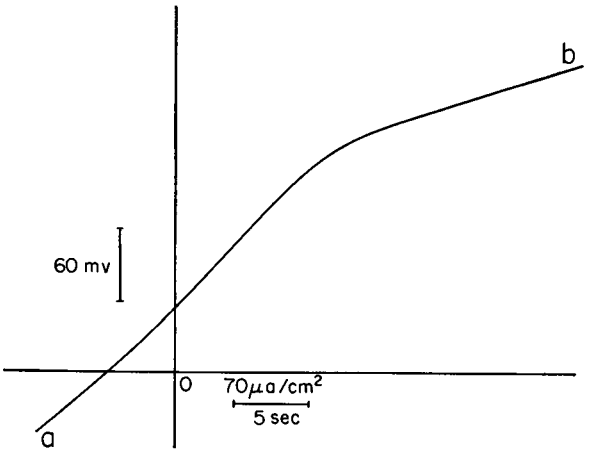


FIGURE 4

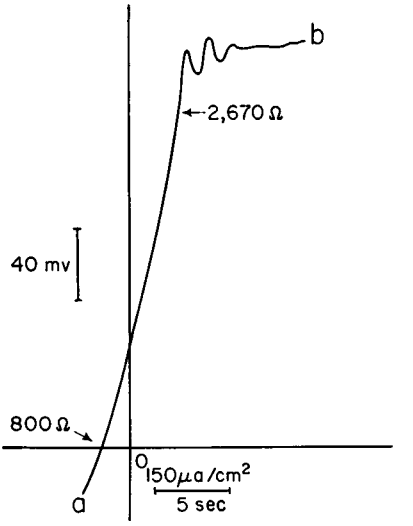


FIGURE 5

FIGURE 4 Recording of an *I-V* relation. Coordinates and scales (potential, current, and time) have been added. Skin bathed in NaCl Ringer's. Curve was started in *a* and ended in *b*.

FIGURE 5 Recording of an *I-V* relation. Coordinates and scales (potential, current, and time) have been added. Skin bathed in NaCl Ringer's. Curve was started in *a* and ended in *b*. Resistances for 1 $cm^2$ of skin are indicated at SCC point and before breakdown.

## RESULTS

### *Resistance Curves with the Slow Current Ramp*

Although the *I-V* curves to be described are referred to as being of the hyperpolarizing region, they actually include a portion of the depolarizing region. Most of the time the sweep was initiated about the SCC point and directed towards the hyperpolarizing region.

*NaCl Ringer's.* Fig. 4 shows a typical *I-V* curve (representative of more than 30 experiments) obtained in NaCl Ringer's solution. It can be seen that between the SCC point and about 200 mv the *I-V* relation is reasonably linear. This finding is consistent with the common observation that the skin resistance is constant within the range SCC-PD. However, at about 200 mv a gradual breakdown occurs. Fig. 5 shows a case in which there is a noticeable increase in the "incremental" resistance,[3] from about 800 Ω-$cm^2$ at the SCC point to 2,670 Ω-$cm^2$ just before breakdown. Such a large variation in resistance in NaCl solutions is found in a small percentage of the skins. In this particular case the breakdown is sharp and followed by oscillations. Occasionally, up to four cycles of damped oscillations were recorded after some of the sharp breakdowns.

*$Na_2SO_4$ Ringer's.* When $Na_2SO_4$ Ringer's was used as the bathing solution

[3] The term "incremental" is used to indicate that the resistance is computed at a certain point of the curve as $dV/dI$. Practically, the slope of the tangent to that point indicates the resistance.

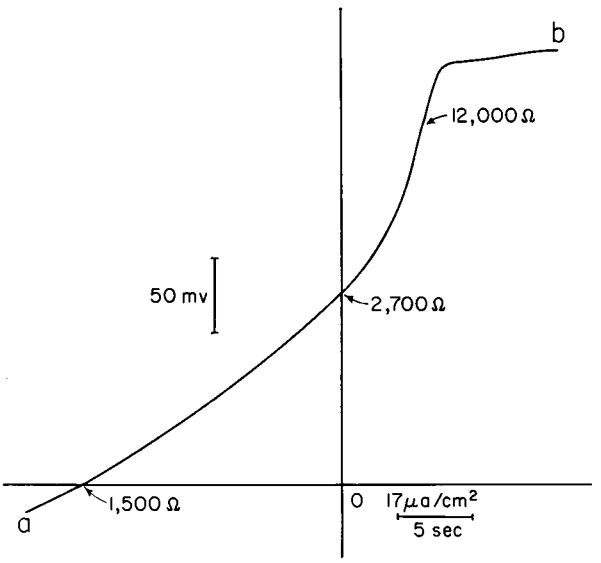


FIGURE 6 Recording of an *I-V* relation. Coordinates and scales (potential, current, and time) have been added. Skin bathed in $Na_2SO_4$ Ringer's. Curve was started in *a* and ended in *b*. Resistances for 1 $cm^2$ of skin are indicated at SCC and PD points, and before breakdown.

on both sides of the skin, the *I-V* relation consistently showed a marked and continuous variation of the resistance. In the hyperpolarizing region just before breakdown, the incremental resistance could be up to 10 times larger than at the SCC point. Also, the incremental resistance at the PD point is usually 1.5 times larger than at the SCC point. The breakdown is always sharp and occurs at a higher level than in NaCl Ringer's, usually at about 300 mv. Much more often than in NaCl Ringer's the breakdown is followed by a region of incremental negative resistance and sometimes by damped oscillations. Fig. 6 shows a typical *I-V* relation in $Na_2SO_4$ Ringer's (this case was selected as representative of more than 50 experiments). The resistance increased 8 times between the SCC point and just before breakdown.

Fig. 7 shows an *I-V* relation obtained in $Na_2SO_4$ Ringer's in which the $Na^+$ concentration was lowered to 31 mM. The general appearance of the curve was similar to the one obtained in $Na_2SO_4$ Ringer's with 104 mM $Na^+$ except that the incremental resistance was proportionally larger at every level and that the breakdown occurred at a higher level, 450 mv in the curve shown in Fig. 7. In some of the experiments, the sweep was reversed after the curve was in progress. If the ramp is reversed before breakdown, the "return sweep" follows the path obtained with the initial sweep. However, if the sweep is reversed after breakdown, as in Fig. 7, the *I-V* relation obtained shows that the resistance is almost linear, as if the breakdown had affected the rectifying property of the skin. It should be pointed out, though, that the effect of the breakdown is not permanent. Similar curves can

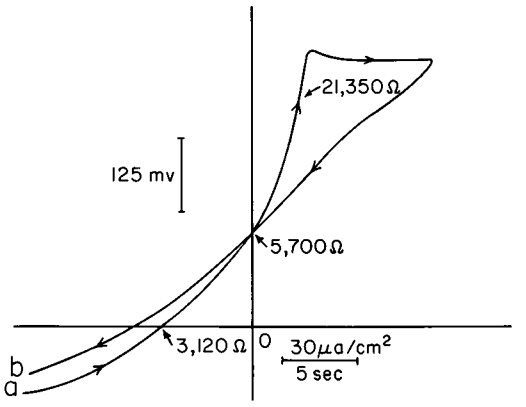


FIGURE 7 Recording of an *I-V* relation. Coordinates, arrows, and scales (potential, current, and time) have been added. Skin bathed in $Na_2SO_4$ Ringer's with a $Na^+$ concentration of 31 mM. Curve was started in *a* and ended in *b*. Notice that the direction of the sweep was reversed after breakdown. Resistances for 1 $cm^2$ of skin are indicated at SCC and PD points, and before breakdown.

be repeatedly obtained for several hours provided that a 1–3 min recovery period is allowed between them.

If the current was held constant after the breakdown had occurred, the potential did not stay constant but decreased to a lower value.

Fig. 7 shows a brief region of postbreakdown negative resistance. This phenomenon was observed in about 40% of the *I-V* curves obtained in $Na_2SO_4$ Ringer's. It is more likely to occur in low $Na^+$ concentrations and in skins with high resistance.

*Choline Chloride Ringer's.* A few experiments were performed in which *I-V* curves were obtained in skins bathed in choline chloride Ringer's. They were found to be very linear with a gradual breakdown occurring at about 300 mv.

*Effect of Some Inhibitors of $Na^+$ Transport.* The effects of nitrogen, $CO_2$, amiloride (amipramizide), and ouabain on the *I-V* relation in the skin were tested. These agents, although acting by different mechanisms, have a common marked inhibitory effect on the PD and the SCC. It was of interest, then, to compare their general effect on the *I-V* relation.

There was a common effect on the *I-V* relation: the incremental resistance at every level of potential went up. There were, however, noticeable differences in how the resistance was increased by each one of the these agents. In the case of ouabain (Fig. 8), even though the PD and the SCC went down, there is still a marked difference between the resistance at the PD point and the maximum resistance just before breakdown. The ratio between these two values (maximum resistance:resistance at PD) was smaller, equal to, or greater than the same ratio in the control curve but always larger than one.

In the cases of nitrogen and $CO_2$ (Figs. 9 and 10), the mentioned ratio was smaller than the control and usually between one and two. To avoid pH gradients, $CO_2$ was bubbled in both bathing solutions. However, its effect was mainly due to its presence in the outside solution.

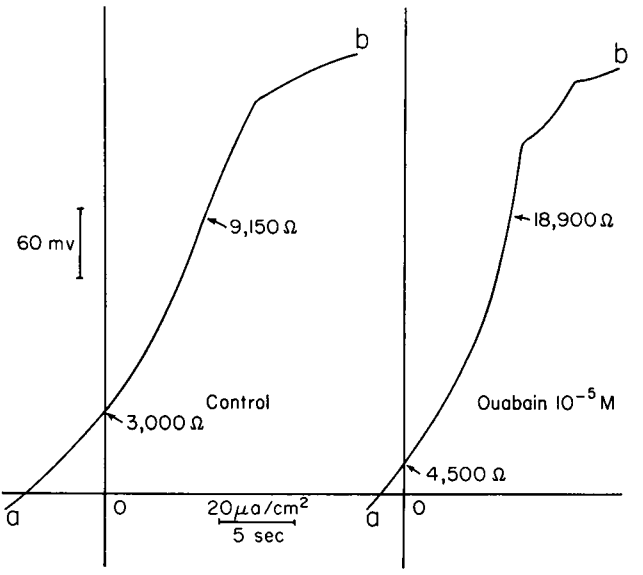


FIGURE 8 Recordings of the *I-V* relation before and after the addition of ouabain to bring the inside bathing solution to a final concentration of $10^{-5}$ M. Skin bathed in $Na_2SO_4$ Ringer's. Curves were started in *a* and ended in *b*. Resistances for 1 cm² of skin are indicated for both curves at PD points, and before breakdown.

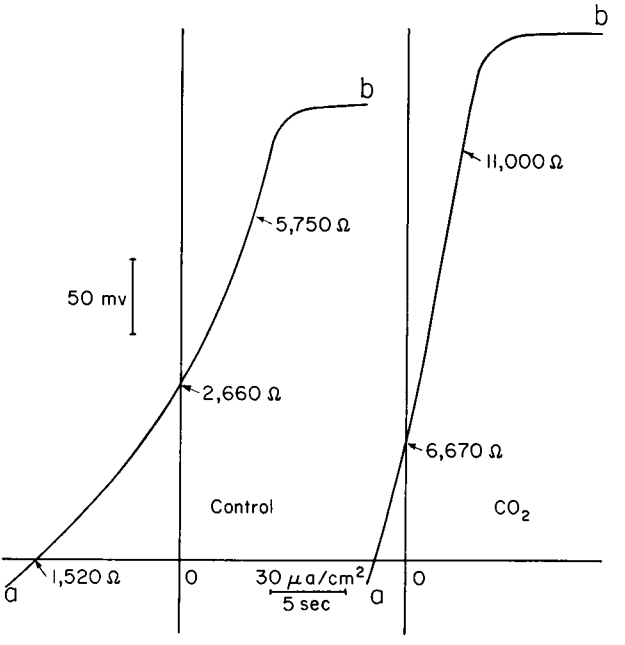


FIGURE 9 Recordings of the *I-V* relation before and after bubbling $CO_2$ in the bathing solutions. Skin bathed in $Na_2SO_4$ Ringer's. Curves were started in *a* and ended in *b*. Resistances for 1 cm² of skin are indicated at various points in both curves.

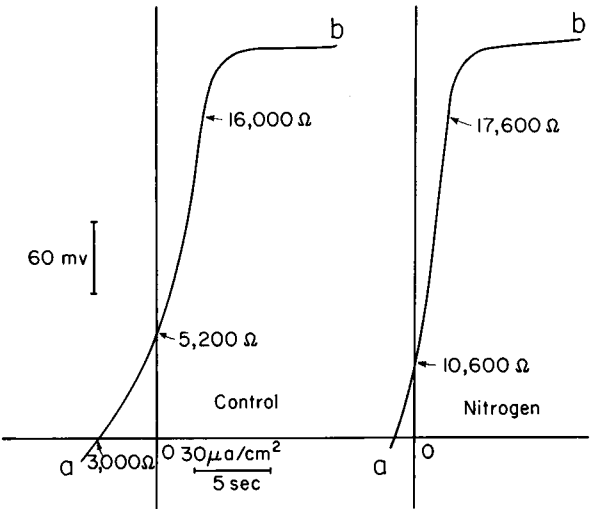


FIGURE 10 Recordings of the *I-V* relation before and after bubbling nitrogen in the bathing solutions. Skin bathed in $Na_2SO_4$ Ringer's. Curves were started in *a* and ended in *b*. Resistances for 1 $cm^2$ of skin are indicated at various points in both curves.

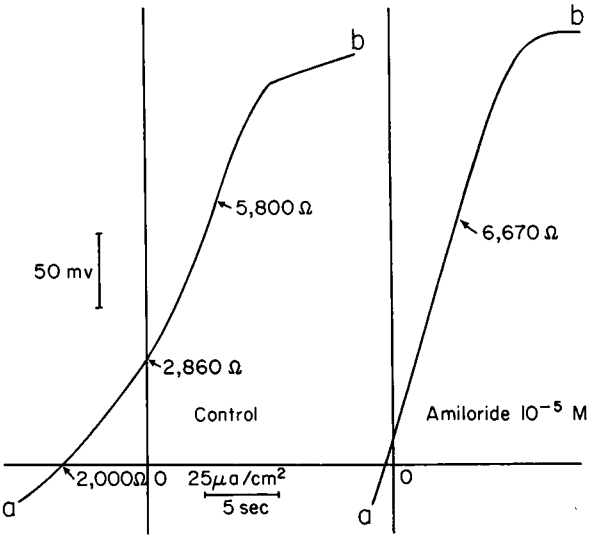


FIGURE 11 Recordings of the *I-V* relation before and after the addition of amiloride to bring the outside bathing solution to a final concentration of $10^{-5}$ M. Skin bathed in $Na_2SO_4$ Ringer's. Curves were started in *a* and ended in *b*. Resistances for 1 $cm^2$ of skin are indicated at various points in both curves.

Amiloride had the quickest and most dramatic effect. In a matter of 1–3 min, the resistance curve was transformed into a straight line (Fig. 11). The four agents, however, had no appreciable effect on the breakdown, except in a few cases where there was a small increase in the potential at which the resistance broke down.

*Resistance Curves with the Fast Current Ramp*

*I-V* curves obtained with the system described in the Methods section as "fast current-clamp ramp" differed in some aspects from those obtained with the *X-Y* recorder used as a slow current ramp. The differences, however, were expected since it is very possible that, due to the capacitance of the skin or to time dependent elements, the speed of the sweep would affect the *I-V* relation. To study this effect, the speed of the sweep was varied from a slow 15 $\mu$a/sec-cm$^2$ (comparable to that used in the slow current ramp) up to a fast 7.5 $\mu$a/msec-cm$^2$. From Figs. 12–18, numbers on the curves indicate different sweep speeds as follows: curve 1, 0.015 $\mu$a/msec-cm$^2$; curve 2, 0.227 $\mu$a/msec-cm$^2$; curve 3, 2.270 $\mu$a/msec-cm$^2$; and curve 4, 7.580 $\mu$a/msec-cm$^2$. However, they do not indicate the order in which they were obtained, although there was always a 10 min interval between them. Fig. 12 shows four consecutive *I-V* relations obtained in NaCl Ringer's. Curves 1 and 1′ were obtained with the same sweep speed, 0.015 $\mu$a/msec-cm$^2$; curve 1 was obtained immediately after the skin was mounted in the chamber and curve 1′, 25 min later. It can be observed that the PD and resistance had increased, which was a common observation in the early part of the experiments, but the breakdown had practically not changed. Curve 3 was obtained 10 min after curve 1′, and curve 4, 10 min after curve 3. It must be noticed that current and voltage scales are the same for all curves in Figs. 12–18, so they can be directly compared. Only the rate at which the current increased was varied.

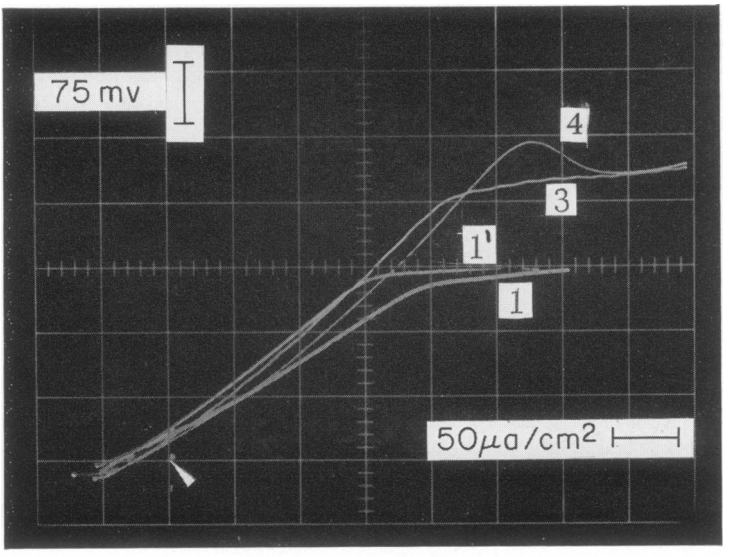


1,1′:3.333 sec; 3:22 msec; 4:6.6 msec

FIGURE 12 Photograph of *I-V* relations obtained at several sweep speeds. Skin bathed in NaCl Ringer's. See description in text. The origin of coordinates is indicated by the pointer. Convention for scales is described in footnote 1.

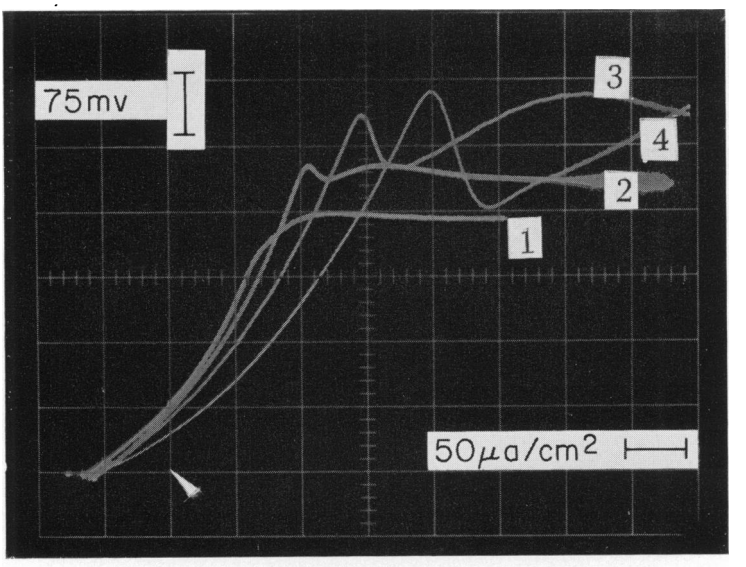


1:3.333 sec; 2:220 msec; 3:22 msec; 4:6.6 msec

FIGURE 13 Photograph of *I-V* relations obtained at several sweep speeds. Skin bathed in $Na_2SO_4$ Ringer's. See description in text. Origin of coordinates is indicated by the pointer. Convention for scales is described in footnote 1.

The main difference between curves 1′ and 3 is that the breakdown occurred at a higher potential in curve 3. Curve 4 shows an even higher breakdown potential and a negative region; also it is shifted to the right with respect to curves 1′ and 3. In general, it can be said that using the slowest sweep speed (15 $\mu$a/sec-cm$^2$), the *I-V* relations are, as they should be, very much the same as those obtained with the *X-Y* recorder. As the sweep speed is augmented, several modifications in the *I-V* relation can be detected: (*a*) the breakdown's potential is elevated; (*b*) a post-breakdown negative region becomes apparent if it was not present at a lower sweep speed or is expanded if it was present; (*c*) the SCC and PD points in the trace do not correspond with those determined under steady-state conditions or using a very slow sweep speed. They moved towards the origin of the coordinates as the whole curve shifted to the right of the plot. It is probable that the skin capacitance is responsible for the variations observed in the *I-V* relation at different rates of current increment. This possibility will be analyzed in more detail in the next section.

Fig. 13 shows the *I-V* relation of the same skin depicted in Fig. 12 when bathed in $Na_2SO_4$ Ringer's. The short-circuit current is about the same as in NaCl Ringer's, the PD is higher (80 mv), and the resistance is higher at every level of potential. Increasing the speed of the sweep produced the characteristic variations observed in all of the *I-V* relations just described in the previous paragraph. Fig. 14 shows the *I-V* curves of the skin in Fig. 13 after $CO_2$ had been bubbled in the chamber for 3 min. The resistance is higher and reasonably linear up to the breakdown except

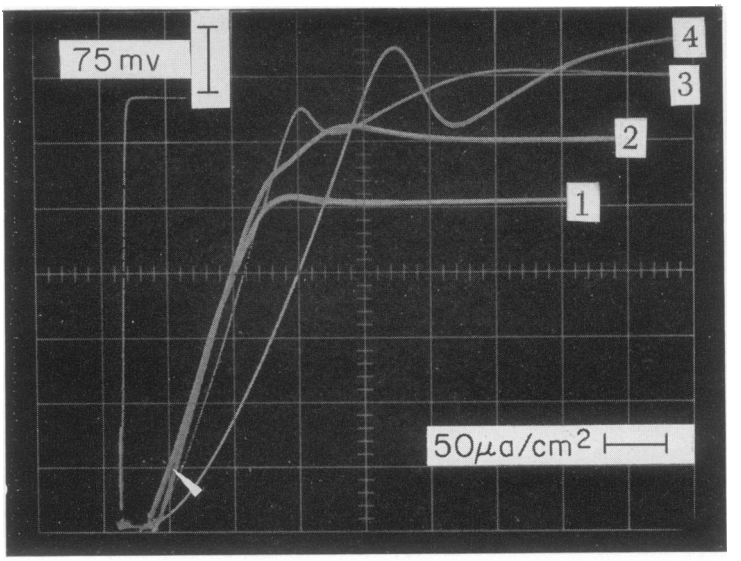


1:3.333 sec; 2:220 msec; 3:22 msec; 4:6.6 msec

FIGURE 14 Photograph of *I-V* relations obtained at several sweep speeds after $CO_2$ was bubbled in the bathing solutions. Compare with curves of the same skin before $CO_2$ bubbling in Fig. 13. Origin of coordinates is indicated by the pointer. Convention for scales described in footnote 1.

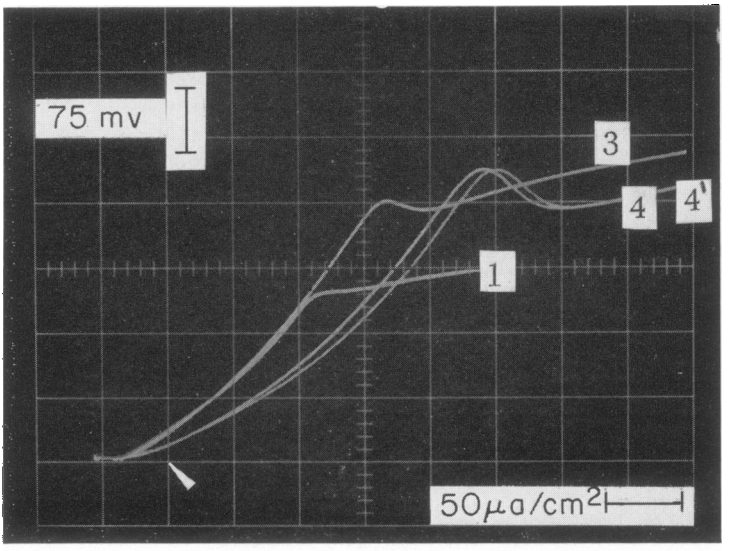


1:3.333 sec; 2:220 msec; 4, 4':6.6 msec

FIGURE 15 Photograph of *I-V* relations obtained at several sweep speeds. Skin bathed in NaCl Ringer's. Notice the similarity between curves 4 and 4' obtained at 30 min interval. Origin of coordinates is indicated by the pointer. Convention for scales is described in footnote 1.

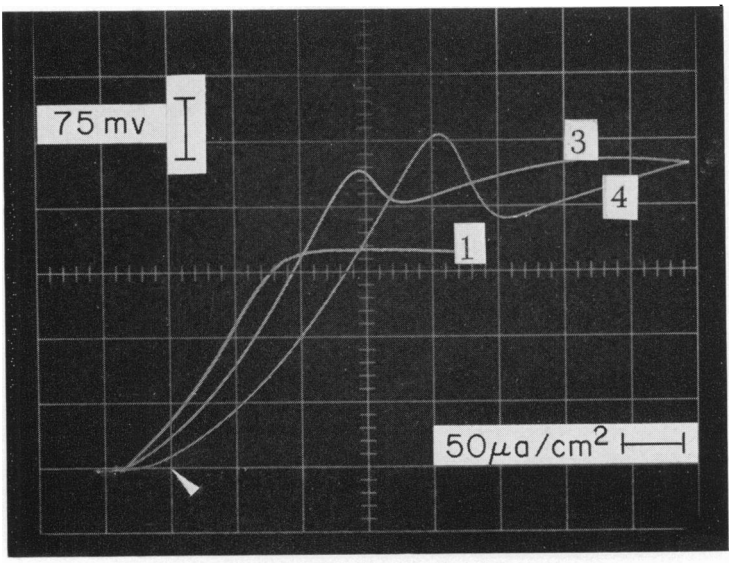


1:3.333 sec; 3:22 msec; 4:6.6 msec

FIGURE 16 Photograph of *I-V* relations obtained at several sweep speeds. Skin bathed in $Na_2SO_4$ Ringer's. Compare them with *I-V* relations of the same skin in Fig. 15.

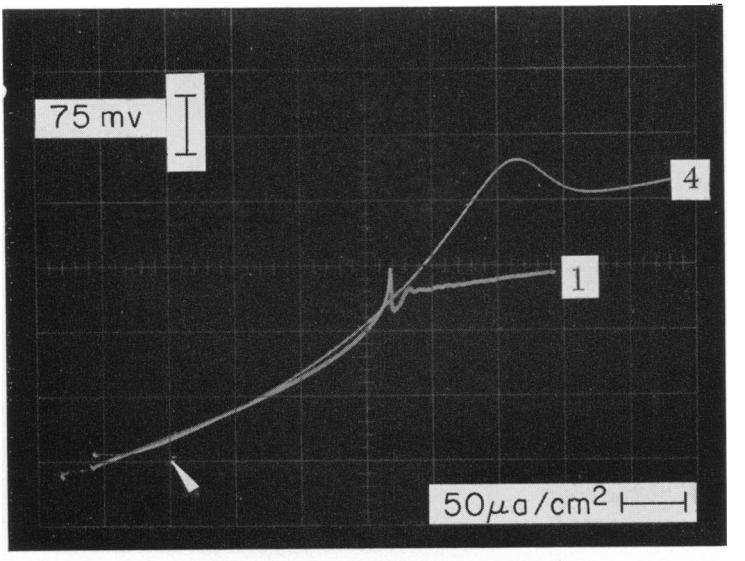


1:3.333 sec; 4:6.6 msec

FIGURE 17 Photograph of *I-V* relations obtained at two sweep speeds. Skin bathed in NaCl Ringer's. Notice oscillations in curve 1.

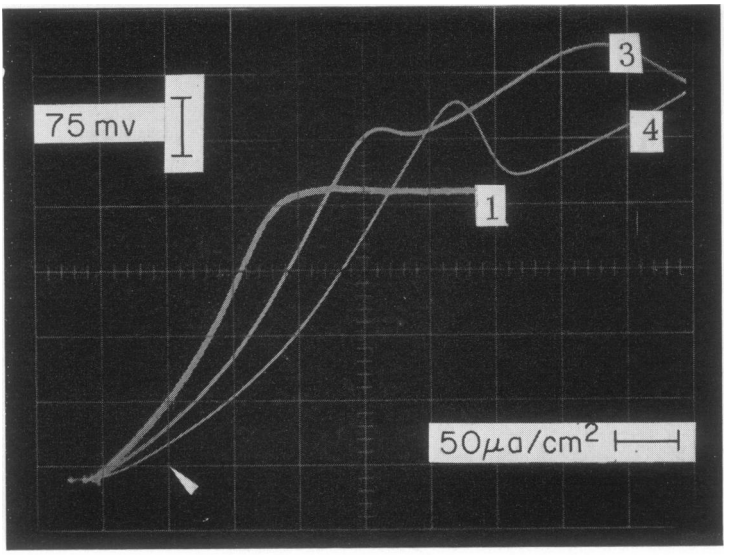


1:3.333 sec; 3:22 msec; 4:6.6 msec

FIGURE 18 Photograph of *I-V* relations obtained at several sweep speeds. Skin bathed in $Na_2SO_4$ Ringer's. Compare them with *I-V* relations of the same skin in Fig. 17.

in curve 4. The curvature at the beginning of curve 4 is probably due to the skin capacitance. The breakdown and negative regions are not affected by $CO_2$. Notice that curves 1, 2, and 3 pass through the origin of the coordinates (spontaneous PD = 0).

Figs. 15 and 16 show *I-V* relations for the same skin; Fig. 15 in NaCl Ringer's and Fig. 16 in $Na_2SO_4$ Ringer's. In Fig. 15 curve 4 was the first one obtained, then curves 1 and 2, and 30 min later, curve 4′. Notice that curves 4 and 4′ are reasonably similar. Figs. 17 and 18 shows curves from the same skin in NaCl and $Na_2SO_4$ Ringer's respectively. There was a 30 min interval between curves 1 and 4 in Fig. 17; also notice the oscillations in curve 1.

### *Unidirectional Sodium Fluxes*

Considering passive ionic fluxes across a diffusion barrier to follow Ussing's relation and Ohm's law, and assuming equal activity on both sides of the membrane, we can write these equations in a simplified form:

$$\frac{\phi_a}{\phi_b} = 10^{(\psi_a - \psi_b)/58.3\ mv}; \qquad \frac{\psi_a - \psi_b}{\phi_a - \phi_b} = R_\phi,$$

where $\phi_a$ is the unidirectional flux of a particular ion which originated in compartment "a"; $\phi_b$ is the flux in the opposite direction; $\psi_a$ and $\psi_b$ the electrical potential in compartments "a" and "b" respectively, $(\psi_a - \psi_b)$ the potential difference across

the membrane, that could be externally applied or generated in the membrane in a parallel pathway; and $R_\phi$ the electrical resistance to the net flux of the ion in consideration. Combining the two previous equations we obtain:

$$\phi_a = \frac{\psi_a - \psi_b}{R_\phi} \left[ \frac{1}{1 - \frac{1}{10^{(\psi_a - \psi_b)/58.3\ mv}}} \right]. \qquad (1)$$

In the limit when $\psi_a - \psi_b$ approaches zero, equation 1 becomes:

$$\lim_{(\psi_a - \psi_b) \to 0} \phi_a = \phi_{a,0} = \frac{58.3\ mv}{R_\phi \ln 10}. \qquad (2)$$

If the PD across the membrane changes from zero to a certain PD, the flux $\phi_a$ should increase or decrease proportionally as given by the ratio $\phi_a : \phi_{a,0}$. For the case in which the PD is changed from zero to +58.3 mv and to −58.3 mv (potential in compartment "a" with respect to "b") the ratio $\phi_a : \phi_{a,0}$ is simply:

$$\frac{\phi_a}{\phi_{a,0}} = \frac{\psi_a - \psi_b}{58.3\ mv} \times \frac{\ln 10 \times 10}{9} = 2.56; \qquad (\psi_a > \psi_b) \qquad (3)$$

and

$$\frac{\phi_a}{\phi_{a,0}} = \frac{\psi_a - \psi_b}{58.3\ mv} \times \frac{\ln 10}{-9} = 0.256; \qquad (\psi_a < \psi_b). \qquad (4)$$

Let's consider $\phi_a$ to be the flux from inside to the outside of the skin (outflux). This flux should be 2.56 times greater than the flux at short circuit when the inside of the skin is 58.3 mv positive with respect to the outside. Conversely, it should be 0.256 smaller when the inside is 58.3 mv negative with respect to the outside.

Table I shows that these ratios are 1.9 or smaller when the inside is 60 mv positive; and 0.36 or larger when the inside is 60 mv negative. These results suggest that the unidirectional flux from the inside to the outside of the skin, at least par-

TABLE I

UNIDIRECTIONAL SODIUM OUTFLUX IN THE SKIN OF *RANA CATESBEIANA*

| [Na] | Potential difference | Outflux |
|---|---|---|
| | | *μeq/hr-cm²* |
| 104 | +60 | 0.26 |
| 31 | +60 | 0.20 |
| 104 | 0 | 0.14 |
| 31 | 0 | 0.11 |
| 104 | −60 | 0.05 |
| 31 | −60 | 0.04 |

tially, cannot be considered to be simply passive diffusion. Table I also clearly shows at every level of voltage clamping, that increasing the sodium concentration more than 3 times produces an increment of only about 1.3. These results strongly indicate the nonpassive nature of the outflux and suggest an interaction between the flux and the membrane. The importance of these results in connection with the *I-V* curves obtained in frog skin is discussed in the next section.

## DISCUSSION

The main conclusions derived from the results reported in this paper are that the *I-V* relation of frog skin in the hyperpolarizing region is not simply linear but voltage dependent and that the nonlinearity of the resistance curve is due to the ability of frog skin to rectify the $Na^+$ current (whether spontaneously circulating or forced across it). This is apparent from both lines of experiments, $Na^+$ fluxes and *I-V* curves.

Current circulating across frog skin is almost entirely carried by $Na^+$ and $Cl^-$ ions. Removal of $Cl^-$ from Ringer's accentuated the non-linearity of the *I-V* relation, whereas removal of $Na^+$ made the *I-V* relation more linear. The fact that $Na^+$ is actively transported by the skin is an indication per se that the $Na^+$ current is the one more likely to be rectified.

This view is supported by Kornacker (13) who concluded that "rectification involved in active transport requires an inherently rectifying membrane component."

The three phenomenon that we have described in this paper, (*a*) rectification for $Na^+$ current, (*b*) breakdown at 300 mv in the hyperpolarizing region, and (*c*) relative independence of the $Na^+$ outflux from the electrical field, show a remarkable resemblance to properties described by Coster for *Nitella* and *Chara australis* and by Mauro (14) for a "junction" formed by juxtaposition of two membranes, one with negative and the other with positive fixed charges. They also concluded that the properties of that membrane are in many respects, including rectification and breakdown, similar to those of a solid-state p-n junction. It is assumed that in double membranes with fixed charges, of opposite sign, the mobile particles are ions while in semiconductor diodes the particles are electrons and holes. The Poisson-Boltzman equation derived by Shockley (15) for this treatment of the p-n junction can also be applied to those double membranes of fixed charges as Mauro and Coster did.

The relative independence of the $Na^+$ outflux from the electrical field resembles the reverse current in a diode, which is constant in spite of wide changes of potential in the reverse bias region. It is needless to say that the $Na^+$ outflux has the proper direction to be comparable to the reverse current.

Based on the unidirectional fluxes data and the electrical analogies between frog skin and a p-n junction, we propose that a realistic electrical model of $Na^+$ transport in frog skin should include a rectifier instead of a linear resistor in the active transport pathway. Before the breakdown the nonlinear character of the *I-V* curve

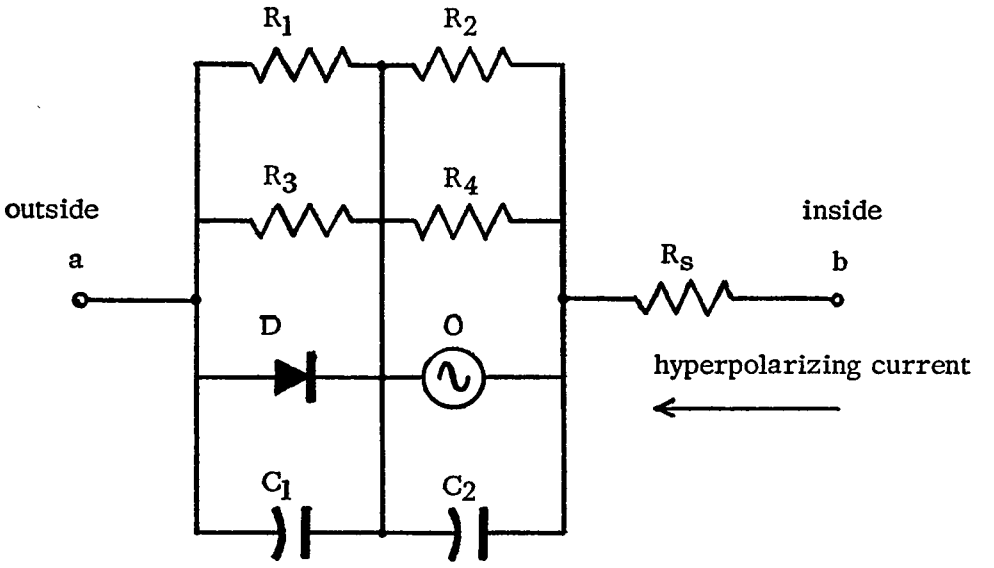


FIGURE 19 Electrical model of frog skin in accordance with data obtained in the hyperpolarizing region of the *I-V* relation. See description in text.

of frog skin in the hyperpolarizing region seems to be due to real rectification and not to a time variant resistance. A time variant resistance will not be adequate to explain our results since rectification is observed with low sweep speeds and with steady-state values of currents. However, the postbreakdown negative region we found can be explained, like the negative region described by Fishman and Macey in the depolarizing region, as due to time variant resistance. An excellent review indicating characteristics of nonlinear resistances has been done by Mauro (16).

To explain our data we feel justified in presenting a different electrical model of frog skin (Fig. 19) in which the main feature is the inclusion of a rectifier. The model can explain most of the electrical results, at least those of the hyperpolarizing region, and the effect of inhibitors described in this paper.

The model consists of three parallel pathways in series with a common pathway. $R_1$–$R_2$ is a passive pathway for anions, mainly $Cl^-$; $R_3$–$R_4$ is a passive pathway for cations which includes the passive fraction of the $Na^+$ flux. D–O is the rectifying pathway for $Na^+$; it includes a rectifier D and an oscillator O. An oscillator is necessary since a diode cannot generate a PD by itself. It also represents the energy source for the active transport of $Na^+$. A battery instead of the oscillator could serve the same purpose, but since the circuit includes a rectifier there is no real necessity for a battery. The three pathways are bidirectional, and without an external electrical field the net fluxes will be from *a* to *b*. $R_s$ is a series resistance representing the connective tissue.

Two main barriers are also depicted in the model: (*a*) an outside barrier consisting

of $R_1$, $R_3$, D, and $C_1$. $C_1$ includes the junction capacitance of the diode; (*b*) an inside barrier consisting of $R_2$, $R_4$, the energy source O and a capacitance $C_2$. It should be noted that the location of the diode of this model is consistent with evidence that the outermost layer of the skin seems to have a selective $Na^+$ permeability, namely: (*a*) excitability and resting potential have been found at that level (6); (*b*) amiloride which seems to affect the diode has a quick and dramatic effect when added to the outside solution; and (*c*) Biber and Curran (17) have recently reported that amiloride blocks $Na^+$ permeability at the outside boundary. In this model the oscillator is placed in the inside barrier consistent with evidence indicating that metabolic processes are not located in the outermost layer of the skin.

The model in Fig. 19 reasonably reproduces the electrical data obtained in frog skin. It shows a spontaneous PD. The *I-V* curve shows a continuous increase of resistance in the hyperpolarizing direction; and as $R_1$–$R_2$ and $R_3$–$R_4$ are eliminated (simulating removal of $Cl^-$ and reduction of $Na^+$) the variation in resistance is accentuated. Also at a certain reverse-bias potential the diode breaks down. As the speed of the sweep is increased the curve shifts to the right (according to our convention of plotting) and the breakdown occurs at a higher potential. These last two phenomena can be explained as follows: at very low speeds the potential across *a–b* is divided between $C_1$, $C_2$, and $R_s$. As the sweep speed is increased, due to capacitances $C_1$ and $C_2$, the potential across *a–b* will lag the current through $R_s$. Consequently, a given potential will require more current as the sweep speed is increased, and a shift to the right will be observed. If the reactance of $C_1$ is larger than that of $C_2$, the voltage drop across $C_2$ will be proportionally larger at higher sweep speeds and a larger voltage difference will be measured across *a–b* for the same breakdown voltage across D.

There are probably many other circuits that can satisfy our results but the one presented here seems to be simple and accurate enough for our present purpose. However, this circuit does not clarify all the questions for which we only have tentative answers. Some of these questions are as follows. (*a*) Can a p–n junction be produced in an organic material? According to Gutmann and Lyons (18), this does not appear feasible for homogeneous material but it is possible to make heterojunctions without a continuous parent lattice. (*b*) How is the coupling between the metabolic energy and the ionic transport accomplished? Blumenthal, Caplan, and Kedem, (19) have devised an ingenious model of transport that demonstrates the possibility of such coupling. It consists of a composite membrane of opposite, fixed charges. The hydrolysis of N-acetyl-L-glutamic acid diamide to ammonium N-acetyl-L-glutamine acts as a "fuel" for the system that gives rise to an electromotive force and a short-circuit current. Kornacker (13) discussed this problem indicating the possibilities of chemical and electrical coupling. (*c*) Why is no AC ripple found, even in the range of microvolts, added to the DC PD? The accepted capacitance of about 1 $\mu F/cm^2$ will require extremely high frequency in the oscillator for a rippleless out-

put. However, the circuit model represents a unit of transport, and there is probably a very large number of them per $cm^2$ with the ripple's phase randomly distributed, thus producing a mutual cancellation. (*d*) What produces the oscillations, post-breakdown negative resistance, and its accentuation by the speed of the sweep? Negative resistance could be a specific characteristic of the rectifier under certain conditions. Also a breakdown in the capacitor $C_2$ just before D breaks down can produce a sudden negativity in the *I-V* curve.

One important difference in the present model with respect to previous ones is that the pump is composed of a combination of two functionally different structures: the "$Na^+$ rectifier" and the energy source. The integrity of both is required for a net transport of $Na^+$. Amiloride, nitrogen, $CO_2$, and ouabain were tested hoping that their effects could expose the elements we have included in the model. Amiloride changed the *I-V* curve (except for the breakdown) to a linear relation of high resistance. Its effect can be interpreted as the foward resistance of the rectifier being greatly increased. The effect of amiloride on $Na^+$ fluxes across the toad skin and toad bladder have been studied by Ehrlich, Crabbe, and Scarlata (20). When SCC is abolished, the "forward" $Na^+$ flux is reduced to a value similar to the "backward" flux. Bentley (21) has suggested that amiloride restricts the entry of $Na^+$ across the mucosal barrier in toad bladder. This idea is consistent with the findings of Biber and Curran in frog skin (17). Although amiloride does not seem to affect metabolic processes and $Na^+$ can still move across the skin in its presence, PD and SCC are totally abolished when the rectifier is impaired by this agent.

Ouabain has a different effect. After PD and SCC were decreased or abolished, the *I-V* curve still showed signs of rectification, although the total resistance of the membrane had increased. Its effect can be electrically interpreted in terms of a disconnection or uncoupling of the "oscillator." $Na^+$ could then move only across the inside barrier via $R_4$.

Nitrogen had an effect similar to that of ouabain. $CO_2$ seems to have a dual effect; Fig. 9 shows a difference between resistance at PD point and maximum resistance. However, in some cases this difference was not apparent and the *I-V* curve resembled that produced by amiloride. Since $CO_2$ bubbling changed the pH of the solution from 8.6 to 6.2, HCl was added to the solution to reproduce an equal change. Due to this pH change the resistance curve suffered a modification similar, but to a lesser degree, to that produced by $CO_2$. The action of $CO_2$ on the electrical model remains unclear but part of it may be due to a pH change.

A detailed quantitative analysis of the components of the model depicted in Fig. 19 seems premature and out of the scope of this paper.

Several lines of experiments are presently in progress in this laboratory in order to reaffirm, modify, or even disprove our present assumptions.

The design and construction of Lucite chambers and part of the electronic equipment was done by Mr. Carl D. Mills, to whom I am greatly indebted; Mr. Mills also provided technical assistance.

This research was partially supported by NIH grant GM 16526 to Dr. Candia; and by NIH grant EY 330 and a Hartford Foundation grant to Dr. Irving H. Leopold.

*Received for publication 10 March 1969 and in revised form 2 October 1969.*

## REFERENCES

1. LINDERHOLM, H. 1953. *Acta Physiol. Scand.* **31**:36.
2. BROWN, A. C., and K. G. KASTELLA. 1965. *Biophys. J.* **5**:591.
3. FINKELSTEIN, A. 1961. *Nature (London).* **190**:1119.
4. FINKELSTEIN, A. 1964. *J. Gen. Physiol.* **47**:545.
5. LINDEMANN, B., AND U. THORNS. 1967. *Science (Washington).* **158**:1473.
6. FISHMAN, H. M., and R. I. MACEY. 1968. *Biochim. Biophys. Acta.* **150**:482.
7. BUENO, E. J., and L. CORCHS. 1968. *J. Gen. Physiol.* **51**:785.
8. FISHMAN, H. M., and R. I. MACEY. 1969. *Biophys. J.* **9**:127.
9. FISHMAN, H. M., and R. I. MACEY. 1969. *Biophys. J.* **9**:140.
10. FISHMAN, H. M., and R. I. MACEY. 1969. *Biophys. J.* **9**:151.
11. COSTER, H. G. L. 1965. *Biophys. J.* **5**:669.
12. CANDIA, O. A. 1966. *I.E.E.E. (Inst. Elec. Electron Eng.) Trans. Bio.-Med. Eng.* **13**:189.
13. KORNACKER, K. 1969. *In* Biological Membranes. R. M. Dowben, editor. Little, Brown and Company, Boston. 39.
14. MAURO, A. 1962. *Biophys. J.* **2**:179.
15. SHOCKLEY, W. 1949. *Bell Syst. Tech. J.* **28**:335.
16. MAURO, A. 1961. *Biophys. J.* **2**:353.
17. BIBER, T., and P. F. CURRAN. *Physiologist.* **12**:176.
18. GUTMANN, F., and L. E. LYONS. 1967. *In* Organic Semiconductors. John Wiley and Sons, Inc., New York. 632.
19. BLUMENTHAL, R., S. R. CAPLAN, AND O. KEDEM. 1967. *Biophys. J.* **7**:735.
20. EHRLICH, E. N., J. CRABBE, AND J. SCARLATA. 1968. *Pflugers Arch. Gesamte Physiol. Menschen Tiere.* **302**:79.
21. BENTLEY, P. J. 1968. *J. Physiol. (London).* **195**:317.